Assessing the influence of CT acquisition parameters on flaw detectability through simulation

Caroline Vienne[1], Julie Escoda[1], Anthony Touron[1], Marius Costin[1]

[1]Université Paris-Saclay, CEA, List, F-91190, Palaiseau, France, e-mail : caroline.vienne@cea.fr

Abstract

X-Ray Computed Tomography (XCT) is a unique tool to fully visualize and understand the nature and size of flaws in industrial parts, with a growing application in different fields such as aeronautics and more recently metal additive manufacturing. The inevitable questions underlying any XCT inspection concern the detectability limit of the measure. What size of defect will be detected with my current configuration? How can I optimize my acquisition material or parameters to improve the detectability limit? Naturally, the known characteristics of the XCT systems (detector pixel size, X-ray tube voltage and focal spot size, magnification) give a first answer to these questions, at least in terms of spatial resolution, but it is more difficult to estimate a priori the visibility of a flaw in terms of contrast. The cost of XCT inspection, the difficulty to design specimen with narrow internal defects and the influence of the geometry of the part on the XCT image quality make experimental analysis of the detectability limits difficult. The simulation brings therefore a promising alternative, provided that it gives a thorough representation of a real inspection.

Keywords: XCT simulation, probability of detection, NDT

1 Introduction

Among the various non-destructive testing (NDT) methods, X-ray Computed Tomography (XCT) is a powerful tool to characterize and localize inner flaws and to verify the geometric conformity of an object. The number of industrial applications of XCT is large and rapidly increasing with typical areas of use in aeronautics [1], aerospace, automotive and energy industries. This technique also benefits from the growing use of metallic additive manufacturing (AM) in these sectors, since it has been established as the most promising technique to inspect AM-produced complex parts [2].

However, it is well known that the quality of the XCT images is influenced by various acquisition parameters such as source voltage and filtration, detector pixel size, magnification, object positioning, number of projections, image averaging. To better understand the influence of these parameters on the detection of flaws, experimental studies have recently been proposed. Hermanek and Carmignato [3] designed a reference object for accuracy evaluation of porosity measurements and conducted an evaluation of the influence of the tube intensity and voltage on the measurements. In [4], Kim et al. proposed another artifact incorporating cubic defects generated by an AM process to study the effect of some acquisition parameters on image quality and probability of detection (POD). The influence of six XCT acquisition parameters was investigated experimentally from a set of twenty experimental runs and the influence of these parameters on the image quality was ranked. Finally the acquired data were used to determine the POD for the given artefact and XCT acquisition parameters.

Probability of detection (POD) is a statistical method applied to NDT to link the probability to detect a critical flaw to its size and is generally used for giving the maximum flaw size that the process can miss with a given level of probability and confidence. The statistical validity of this approach is highly dependent on the amount of data available, which makes numerical simulation a great asset thanks to its ability to give a very large amount of data at a relative low cost. The so-called “Model Assisted” POD approach has been integrated in CIVA, the multi-technique Non Destructive Testing (NDT) simulation software developed by CEA List [5,6]. On top of providing data for POD curves, simulations and metamodels can also be used at the design stage to optimize inspection methods and procedures for detecting a given flaw size. More generally, simulation is a great asset for conducting extensive studies on parameters influence on the result quality.

In this paper, we present in detail the XCT module of CIVA and how it can be used to both choose the best parameters to maximize the detectability of a given flaw and assess the detectability limit of a given configuration. A 3D detectability criterion is proposed and will be integrated in the next versions of CIVA to establish probability of detection curves.

2 Simulation of CT inspection with CIVA

CIVA is a multi-technique NDT simulation software [7], which integrates a radiographic and computed tomographic (RT/CT) module, allowing the modeling of a complete inspection chain for X-ray CT. It provides a user-friendly graphical user interface

https://doi.org/10.58286/26621

(GUI) to define all parameters necessary for the simulation and relies on a simplified model of photon-matter interaction allowing a reduced computation time without loss of image fidelity.

2.1 Modeling photon-matter interactions

The X-ray simulation code models the physics of photon-matter interaction in the range of 1 keV to 100 MeV, through the three most important processes: photoelectric effect, scattering (coherent and incoherent) and pair production. A fast computation of the attenuation is performed with the Beer-Lambert law, to which a Monte Carlo computation is combined in order to estimate the scattering phenomena. Distinct images are computed and combined into a final one, which also integrates the influence of the X-ray source (size, spectrum and filtering), the photonic noise and the detector response (modulation transfer function, noise model).

2.1.1 Analytical computation: direct beam

This fast computation is applied to every ray connecting each pixel of the detector and the source point. The list of intersections of the ray with the objects of the scene is first established, then the list of thicknesses of the different materials crossed by the beam is used to compute the attenuation of the incident X-ray spectrum through the Beer-Lambert law. Finally, the transformed spectrum reaching the detector is converted into a deposited energy.

2.1.2 Monte Carlo computation: scattered beam

This additional statistical computation is required in the configurations where the scatter contribution is important. A large number of photons is emitted randomly in the X-ray cone beam and each photon is tracked along its path through the matter until it is fully absorbed, reaches the detector, or is lost. The mean free path of the photon between two interactions within a material, known from its energy and the characteristics of the matter, gives the displacement of the photon before its next interaction. The nature and effect of this interaction is then computed statistically and applied to the photon. It is the most time consuming step of the simulation process but, contrarily to full Monte Carlo particles transport codes such as PENELOPE [8], the objective in CIVA is only to have enough photons on the detector to have a rough estimation of the scatter contribution, which is a low frequency signal. This scatter signal is then smoothed before being added to the analytical deposited energy.

2.2 Defining the acquisition parameters

All the elements of the acquisition setup are successively defined in the different window tabs in an industrial point of view. Figure 1 presents the CIVA GUI of a typical CT configuration with a circular trajectory. A preview of the created CT scene is displayed in the right window. The blue dots represent the positions of the source with respect to the object during the CT acquisition. The green square represents the detector in the first position and the emission cone is displayed in yellow. It is also possible to trace the paths of 50 photons emitted from the source to have a rough idea about the transmission and whether scattering can be neglected. If none of the 50 photons traced reach the detector, scattering beam is likely dominant, and a direct radiation calculation will not be sufficient.

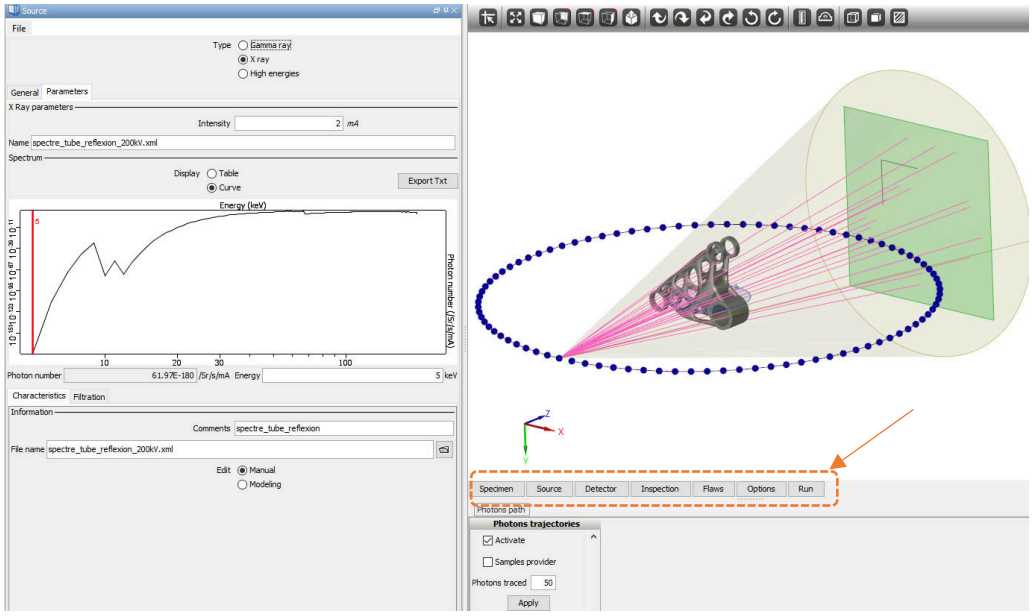

Figure 1: Overview of CIVA CT scene. Display of the parameters of the X-ray source (left) and visualisation of the acquisition trajectory and photon paths (right)

From the lower part of this active model window, the user selects the different elements of the inspection (see orange arrow in Figure 1) to open a left panel, in which the parameterization of this element is done.

- ***Specimen (and Flaws)***

The object to inspect is defined as a simple parametric object (plane, cylinder, elbow, weld…) or using a CAD model (supported formats are stp, igs and stl) and flaws of different shapes can be included and positioned inside it. In addition to the geometry of the part, it is possible to define here its material (simple material or alloy) and its position and orientation in the CIVA global frame. Multiple objects and flaws can be represented with their own characteristics (material and position).

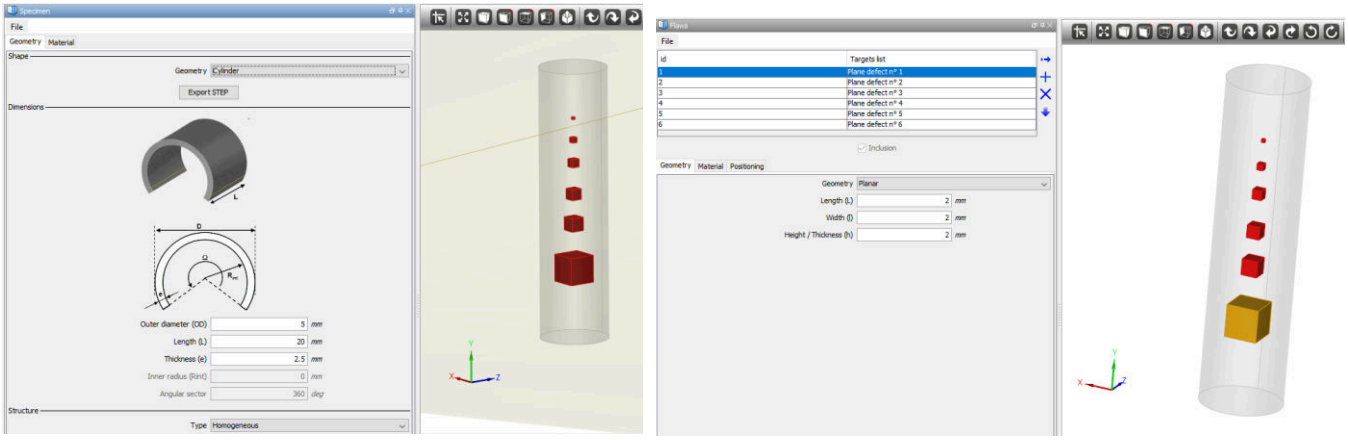

Figure 2: Definition of a cylindrical specimen of diameter 5 mm (left) and insertion of six internal cubes of different nominal edge length in (right).

- ***Source***

From the Source window, the user can choose the nature of the source (Gamma, X-ray tube or linear accelerator). In the general case of XCT, the X-ray tube is considered and defined by its spectral distribution, which can be obtained by loading a precomputed spectrum obtained with a Monte Carlo simulation (see Figure *1*), by loading a text file (*.dat / *.txt) of experimental values or by using the spectrum calculator. Additional parameters of the source include the filtration and the size of the focal spot. This last parameter is essential to model the geometric blur due to the source.

- ***Detector***

Among the six types of detectors available in CIVA (Digital radiography, scintillator with CCD, tape-film, NF EN ISO 11699-1 film, image plate or generic detector), the Digital radiography model corresponds to the classical flat panels widely used in XCT. It is parametrized by the number and size of its pixels, the thickness and material of the scintillator and a global gain corresponding to the transformation of the deposited energy into a measurable signal. It is also possible to model the input window of the flat panel by a pre-filter and the intrinsic blur by a Modulation Transfer Function (MTF) calibrated by importing an experimental curve or by generating a MTF curve using a spatial resolution value (twice the size of the pixel by default).

- ***Geometry***

In CIVA, the source and the detector are mobile, and the object to be inspected is stationary, which allows to better visualize the acquisition trajectory, displayed as blue dots corresponding to the successive positions of the X-ray source (see Figure *1*, left). Circular, multi-circular, helical, semi-helical or specific trajectories can all be considered in CIVA. The first ones are parametrized by the distances between the source and detector (SDD) and the source and the object (SOD), the number of views, the angular step and the pitch, while the last one is defined by loading a text file describing the list of source and detector positions and orientations.

2.3 Reconstruction algorithms

Several reconstruction algorithms are implemented to obtain the 3D reconstructed data from the set of simulated radiographies. For dense circular trajectories, the standard FDK algorithm [9] is the gold standard in 3D reconstruction because of its good results in reasonably short reconstruction time. For non-standard trajectories or sparse sampling, iterative algorithms (SART, SIRT) are also available with a GPU card. The reconstruction is possible for the whole specimen or a region of interest and displayed by a 3D rendering and three orthogonal slices (see Figure 3)

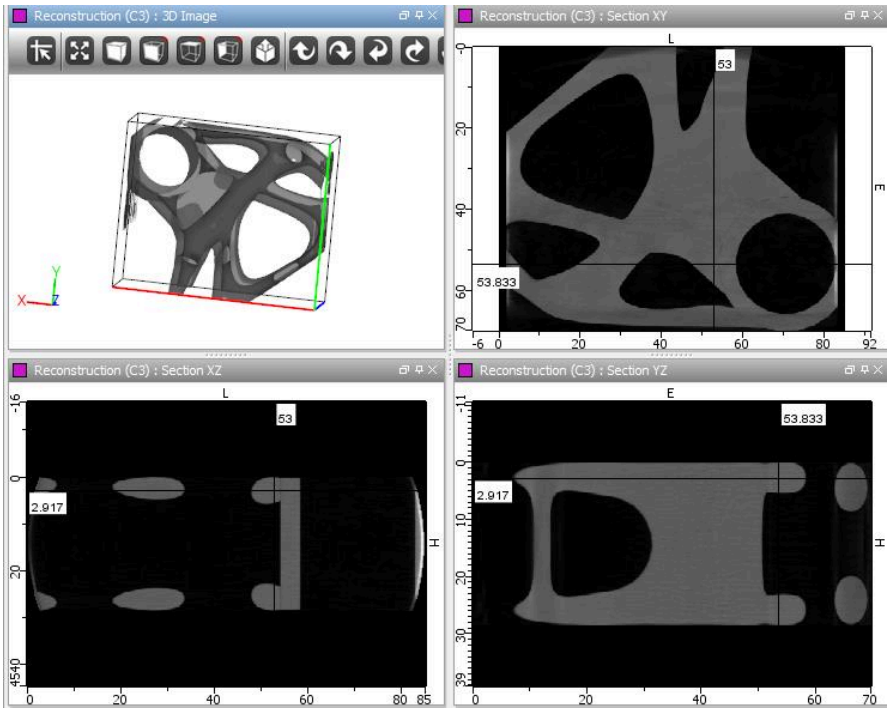

Figure 3: Visualisation of the reconstruction result by its isosurface and three orthogonal planes.

2.4 Variation and POD capabilities

The Variation tool is available for all techniques in CIVA in order to perform parametric studies. To define a Variation scenario, the user selects the parameter(s) that will vary and their variation range. Then, the corresponding batch of simulations is run and several extractions can be applied to each resulting image in order to monitor the influence of the considered parameters.

POD curves are estimated in CIVA using the Maximum Likelihood Estimation methods recommended in the MIL-HDBK 1823A [10] for Hit-Miss and Signal Response data. The simulation-POD approach implemented in CIVA follows the uncertainty propagation method, which consists in:

- Defining a characteristic parameter for POD computation (typically the flaw size)
- Defining parameters to vary within the range of the studied procedure,
- Describing uncertainty distributions for each of the uncertain parameters,
- Launching computations corresponding to Monte-Carlo sampling of the uncertain parameters,
- Analyzing the resulting data set and compute POD curves.

The POD framework is already available in CIVA for radiographic inspection [11] and will be adapted to CT analysis in the next releases of the software.

2.5 Validation of the models

With the ambition to replace experimental analysis and POD by simulation results, it is essential to validate that the results obtained with CIVA simulations are reliable and accurate. This validation consists in evaluating the reliability/accuracy of its predictions by comparing these predictions to reference results, coming either from experiments on mock-ups (experimental validation), or using other codes or models such as full Monte Carlo codes [8]. Such validation studies have been published in the past [12], as well as case studies where the performances of different NDT techniques are compared through simulation [13].

3 Simulation study and results

As a first step towards Probability of Detection studies of Computed Tomography using CIVA, we present here a parametric variation of different acquisition parameters of the CT setup (scene geometry, trajectory, X-ray source, etc…) and their influence on the detectability of a given flaw. One of the new functionality of CIVA 2021 concerns the application of the reconstruction algorithm (FDK) directly following the generation of the simulation results. Therefore, when running batches of simulation, it is now possible to access the 3D image in addition to the set of radiographic images. As a further step, we aim at integrating a detectability criterion applied to such 3D image, similar to the 2D “Rose” criterion already implemented in CIVA for radiographic configurations [14].

3.1 Defining a detectability criterion

The objective of a detectability criterion is not to automatically detect a flaw in a reconstructed image but rather to quantify the detectability of an existing flaw in this image. We use the knowledge of the flaw we have modeled, such as its shape and location in the 3D volume, to build our new criterion. The proposed criterion involves the contrast value μ (mean grey value difference between the flaw and its neighborhood), the noise $\boldsymbol{\sigma}$ and a weighting factor **w** linked to the size of the flaw (maximum dimension) in terms of voxels.
These values can be estimated from the histogram and intensity profile in the reconstructed image (see Figure 4) and the proposed criterion is expressed as follows:

$$\boldsymbol{C = \mathrm{w} \cdot \mathrm{SNR}, \quad with\ \mathrm{w} = \begin{cases} 0,2 & \text{if flaw size} < 3 * \text{voxel size} \\ 0,5 & \text{if flaw size} < 5 * \text{voxel size} \\ 1 & else \end{cases} \quad and\ \mathrm{SNR} = \frac{\mu}{\sigma}}$$

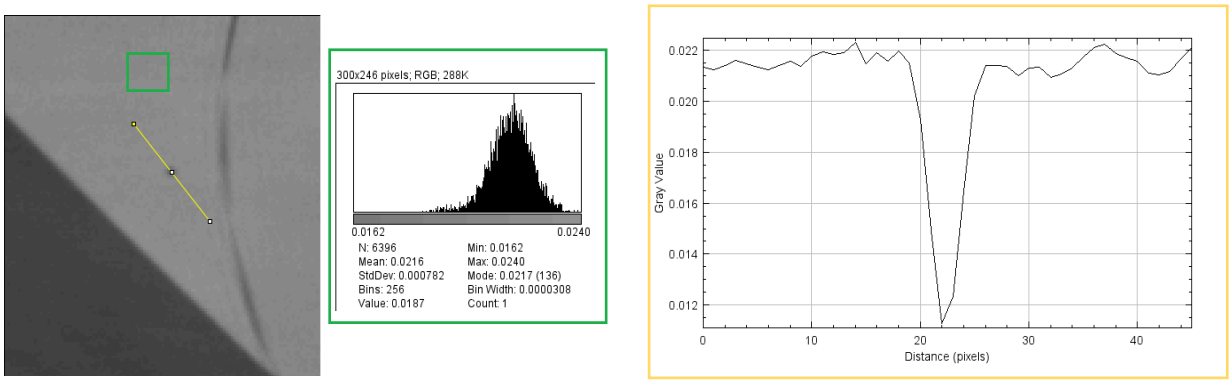

Figure 4: Left, visualisation of the simulated flaw in the reconstructed image. Center, computation of the background noise value from the green rectangle. Right, measure of the grey values of the flaw and background respectively from the profile plotted along the yellow line.

3.2 Using simulation for the optimization of the acquisition parameters

We consider here a classical CT configuration for the NDT inspection of a complex aluminium part coming from Additive Manufacturing (see Figure *1*), in which we insert a porosity of diameter 300 µm. We investigate the influence of the X-ray spectrum by modifying together the maximum voltage and the filtration of the X-ray tube. Figure *5* shows one slice of the CT reconstruction result around the region of interest of the inserted flaw for three configurations corresponding to different X-ray source parameters. The detectability criterion **C** computed on these images is displayed for each configuration and gives a first estimation of the best X-ray settings for the detection of this porosity.

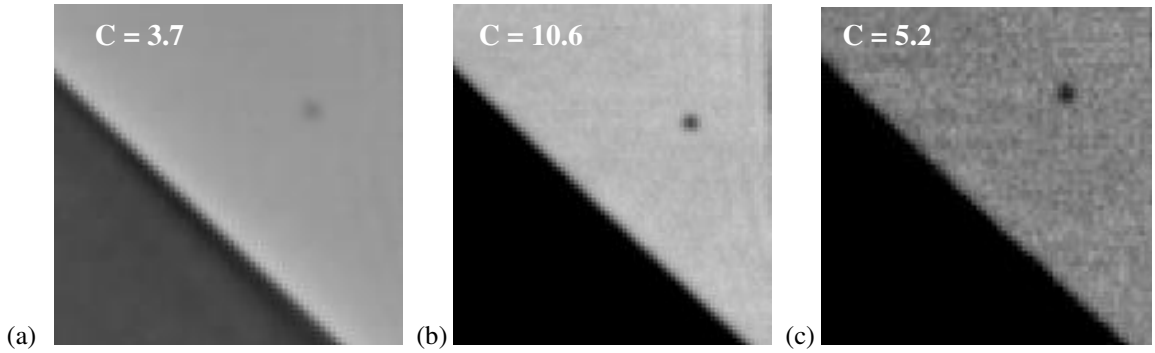

(a) (b) (c)

Figure 5: CT reconstruction results obtained with three different source tension / filter, respectively 100 kV without filter (a), 150 kV with 0.5 mm Cu (b) and 200 kV with 0.5 mm Ta (c)

In a second step, based on the optimal settings for the X-ray tube (150 kV with 0.5 mm Cu), we change the magnification of the setup, placing the object respectively closer to the detector (configuration a) and closer to the source (configuration b). This affects the magnification of the configuration and hence the size of the reconstructed voxel. The voxel size is then 120 µm in configuration a), 80 µm in configuration b) and 50 µm in configuration c). Quite naturally, we notice the improvement in the detectability of the defect with the reduction of the voxel size (see Figure 6).

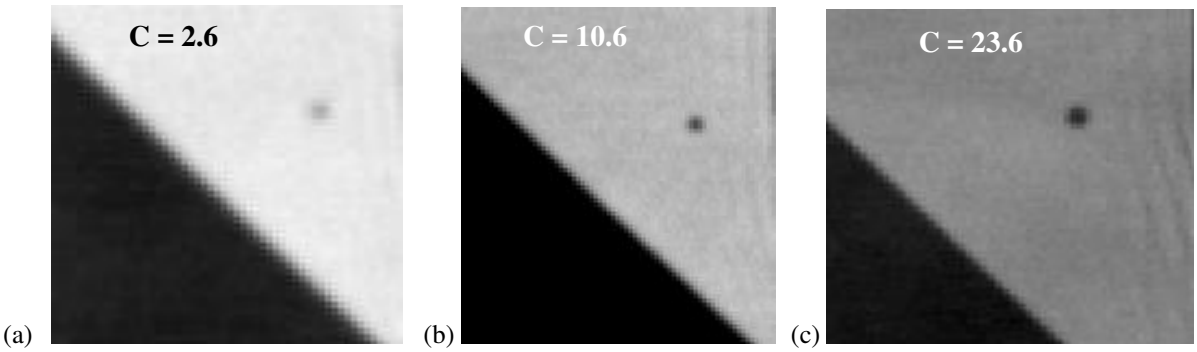

(a) (b) (c)

Figure 6: CT reconstruction results obtained with three different voxel size (different magnification). (a) 120 µm, (b) 80 µm, (c) 50 µm.

3.3 Using simulation for the identification of a limit of detectability

In this second use case, we integrate in a cylindrical part of 5 mm diameter, inspired by the reference specimen proposed in [4], several hollow cubes of increasing size. The material of the part is stainless steel 316L, seven cubes are filled with metal powder and one small one is empty (see Figure 7). A classical CT configuration is simulated with CIVA, using an X-ray tube of 200 kV with 1 mm Cu filter, a detector of 1024 x 1024 pixels with a pixel of 150 µm and a magnification of 7. The metal powder is represented by a homogeneous material with the chemical composition of the 316L steel but a density of 4 g.cm^{-3} (while the density of the part is 7.96 g.cm^{-3}).

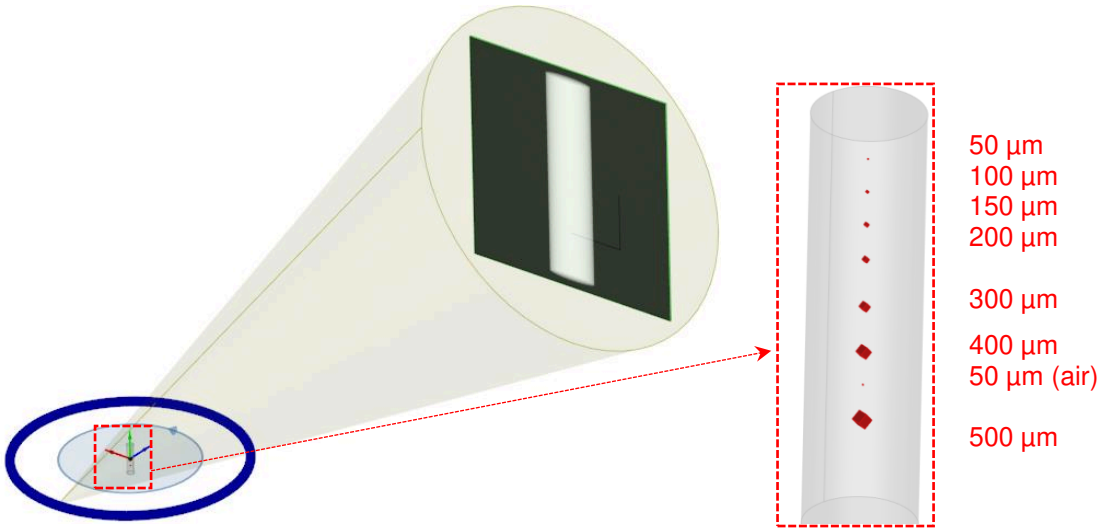

Figure 7: Simulation of a CT configuration for assessing the limit of detectability of a flaw in an AM built part.

The central slice of the reconstructed volume is displayed in Figure 8. For each flaw, the size is indicated, as well as the value of the detectability criterion. In addition, we present the plot of the intensity profile along the flaws. We can notice a saturation of the criterion, which is directly linked to the saturation of the contrast value. For the flaws larger than 300 µm, the attenuation of the powder is well reconstructed and the contrast of the flaw comes from the difference between the attenuation of the powder and the attenuation of the dense matter.

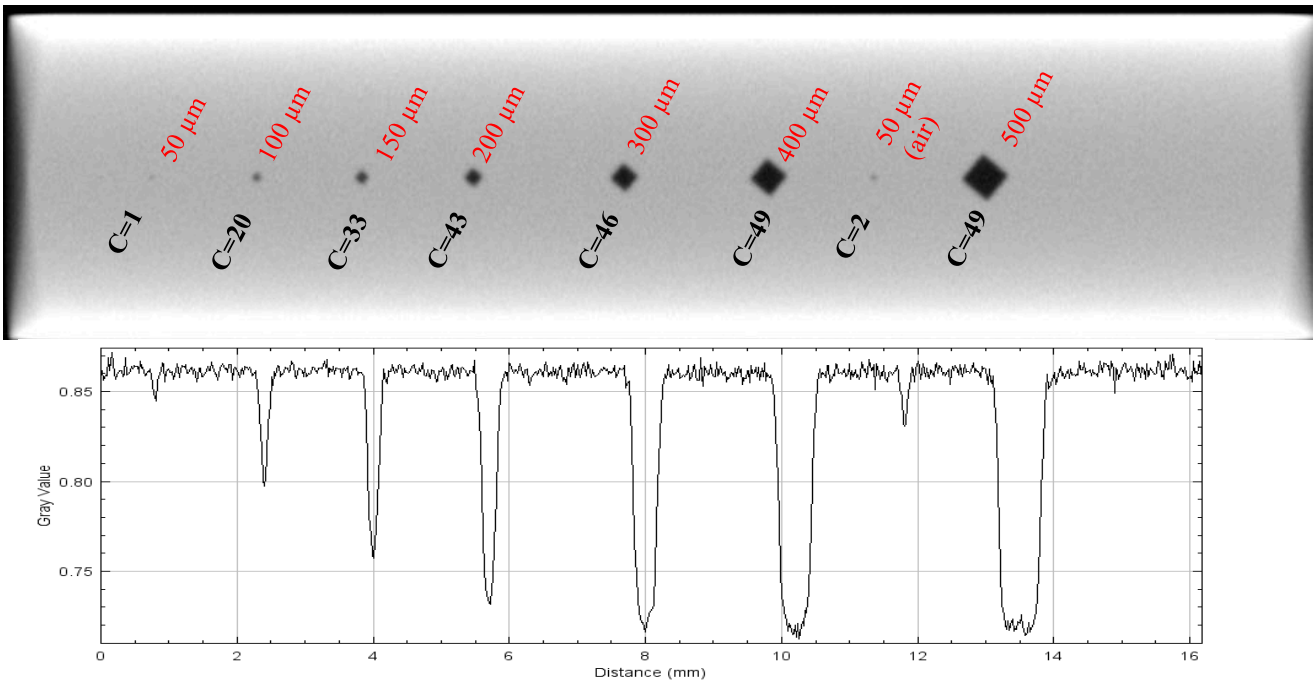

Figure 8: Cross-section of the XCT volume (top) and gray value intensity profile along the flaws (bottom)

4 Conclusion

We present here the potential of using X-ray simulation for conducting a first assessment of the detectability of a specific flaw in a part, based on the chosen X-ray settings, but also for helping in the optimization of the X-ray parameters. In this work, a detectability criterion is proposed and applied on simulated results obtained with CIVA. This is a first step in the deployment of a POD module dedicated to CT configurations, which represents a great opportunity to explore deeper and more precisely some parameters variability and influence that can be difficult to monitor in an experimental study.

References

[1] A. du Plessis, P. Rossouw, X-ray computed tomography of a titanium aerospace investment casting, Case Studies in Nondestructive Testing and Evaluation, Volume 3, 2015, Pages 21-26.
[2] A. Thompson, I. Maskery, R. Leach, X-ray computed tomography for additive manufacturing: A review. Measurement Science and Technology. 27. 072001. 10.1088/0957-0233/27/7/072001. (2016).
[3] P. Hermanek, S. Carmignato, Reference object for evaluating the accuracy of porosity measurements by X-ray computed tomography. Case Studies in Nondestructive Testing and Evaluation. 6. 10.1016/j.csndt.2016.05.003. (2016).
[4] F. Kim, A. Pintar, S. Moylan, E. Garboczi, The Influence of X-Ray Computed Tomography Acquisition Parameters on Image Quality and Probability of Detection of Additive Manufacturing Defects, Journal of Materials Processing Technology, (2019)
[5] F. Jenson, E. Iakovleva, N. Dominguez, Simulation supported POD: methodology and HFET validation case, in Review of Progress in QNDE, 30, 2010.
[6] F. Foucher , R. Fernandez , S. Leberre , P. Calmon, New tools in CIVA for Model Assisted Probability of Detection (MAPOD) to support NDE reliability studies
[7] M. Costin, H. Banjak, C. Vienne, D. Tisseur, R. Guillamet, R. Fernandez, CIVA CT, an advanced simulation platform for NDT, ICT2016, Wels
[8] F. Salvat, J. Fernández-Varea, J. Sempau, Penelope. A code system for Monte Carlo simulation of electron and photon transport. NEA Data Bank, Workshop Proceeding, Barcelona. 4-7. (2007).
[9] L.A. Feldkamp, I.C. Davis, J.W. Kress. Practical cone-beam algorithm. J. Opt. Soc. Am. A, 1(6):612–619, 1984.
[10] MIL-HDBK-1823, Department of Defense Handbook: nondestructive evaluation NDE system, reliability assessment, 1999.
[11] D. Tisseur, M. Costin, B. Rattoni, C. Vienne, A. Vabre, G. Cattiaux, T. Sollier, Experiment vs Simulation RT WFNDEC 2014 Benchmark : CIVA Results, Review of Progress in Quantitative Non Destructive Evaluation, july, 2014, Boise, USA
[12] D. Tisseur, M. Costin, S. Fournier, C. Reece, A. Schumm, POD calculation on a radiographic weld inspection with CIVA 11 RT module, 10th International Conference on NDE in Relation to Structural Integrity for Nuclear and Pressurized Components, 1-3 October 2013, Cannes, FRANCE (JRC-NDE 2013)
[13] M. Papanaboina, D. Cirtautas, A. Asokkumar. Numerical Simulation of Additively Manufactured Metal Component, 12th Symposium on NDT in Aerospace, 2020, Williamsburg, VA, USA
[14] D. Tisseur, C. Vienne, P. Guérin, A. Peterzol Parmentier, V. Kaftandjian, P. Duvauchelle, A. Schumm, A Modified Detectability Criterion for Conventional Radiography Simulation, WCNDT 2016, Munich.